ISSN: 2447-3359

REVISTA DE GEOCIÊNCIAS DO NORDESTE

Northeast Geosciences Journal

v. 11, nº 1 (2025)

https://doi.org/10.21680/2447-3359.2025v11n1ID38917

Composition of an exploratory hydraulic transmissivity map using the parameter transverse electrical resistance

Composição de uma cartografia de transmissividade hidráulica exploratória com a utilização do parâmetro resistência elétrica transversal

Álvaro Luís Patriota Lima Magalhães[1]; Leandson Roberto Fernandes de Lucena[2]

[1] Postgraduate Program in Geodynamics and Geophysics -PPGG/UFRN, Natal/RN, Brazil. Email: luis.lima701@ufrn.edu.br
ORCID: https://orcid.org/0009-0003-6002-7766

[2] Postgraduate Program in Geodynamics and Geophysics -PPGG/UFRN, Natal/RN, Brazil. Email: leandson.lucena@ufrn.br
ORCID: https://orcid.org/0000-0002-7713-861X

Abstract: The Barreiras Aquifer, unconfined in hydraulic nature, has a high hydrogeological potential and supplies approximately 80% of the cities along the eastern coast of Rio Grande do Norte, Brazil. In this context, the research area is located on the left bank of the Boa Cica Stream, in Nísia Floresta, RN. This study aimed to develop an exploratory hydraulic transmissivity (T) map based on aquifer test data and the geoelectric parameter of transverse electrical resistance (RT), the latter obtained from inverse models of vertical electrical soundings (VES). Additionally, sub-areas with higher hydrogeological potential were characterized based on the direct correlation between RT and T. The results demonstrated the satisfactory application of this methodology for determining transmissivities from transverse resistance, provided that prior hydrogeophysical calibration is considered, involving lithological-constructive profiles, aquifer testing, and the inverse model of the VES performed adjacent to the well. The highest RT values were identified in the central and western sub-areas, reaching 58,860 Ohm.m², associated with greater hydrogeological potential zones. In this regard, the analysis of the predominant factor in the calculation of RT, through linear regression, revealed an R^2 coefficient of 0.89, highlighting the predominance of the aquifer's average resistivity (linked to its hydraulic conductivity) over its thickness in RT values.

Keywords: Hydraulic transmissivity; Transverse electrical resistance; Unconfined aquifer.

Resumo: O Aquífero Barreiras, de caráter hidráulico não confinado, possui elevado potencial hidrogeológico, abastece aproximadamente 80% das cidades do litoral oriental do Rio Grande do Norte-Brasil. Nesse contexto, a área de pesquisa situa-se na margem esquerda do Riacho Boa Cica, Nísia Floresta-RN. A presente pesquisa objetivou elaborar uma cartografia de transmissividade hidráulica-T exploratória a partir de dados de testes de aquífero e do parâmetro geoelétrico resistência elétrica transversal-RT, este último proveniente de modelos inversos de sondagens elétricas verticais-SEVs. Adicionalmente, subáreas com maiores potencialidades hidrogeológicas foram caracterizadas, com base na correlação direta entre RT e T. Os resultados evidenciaram o emprego satisfatório dessa metodologia de composição de transmissividades a partir da resistência transversal, desde que considerando uma calibração hidrogeofísica prévia, envolvendo perfil litológico-constutivo, teste de aquífero e modelo inverso da SEV executada adjacente ao poço. Os maiores valores de RT foram caracterizados nas subáreas central e oeste, atingindo 58860 Ohm.m², sendo estas associadas a zonas de maiores potencialidades hidrogeológicas. Nesse aspecto, a análise do fator preponderante no cálculo de RT, através de regressão linear, revelou um coeficiente R^2 de 0,89, evidenciando a preponderância da resistividade média do aquífero (associado com sua condutividade hidráulica), em detrimento da sua espessura, nos valores de RT.

Palavras-chave: Transmissividade hidráulica; Resistência elétrica transversal; Aquífero não confinado.

Received: 22/01/2024; Accepted: 08/04/2025; Published: 17/04/2025.

1. Introduction

Hydrogeological and hydrogeophysical studies have become essential in developing reliable strategies for the exploratory management of groundwater resources. This is due to the growing demand for public water supply in large urban centers and the agricultural sector and the need to support regions that face seasonal water shortages. In this context, geophysical studies—particularly those using geoelectrical methods—are crucial for determining the geometry of aquifers and identifying areas more suitable for water extraction, especially in locations lacking well data.

Considering a model of parallel-layered strata, surveys using the electrical resistivity method—particularly the Vertical Electrical Sounding (VES) technique—are highly relevant for studies involving clastic aquifers, as they allow for distinguishing resistivity variations with depth. Additionally, the Dar Zarrouk geoelectrical parameter, known as transverse electrical resistance (RT), has the potential to play a fundamental role in identifying favorable areas for future water extraction, also providing estimates of hydraulic transmissivity (ORELLANA, 1972; SILVA & LUCENA, 2021).

The Barreiras Aquifer, the focus of this research, covers a significant portion of the eastern coast of the State of Rio Grande do Norte, in northeastern Brazil, and is recognized for its high hydrogeological potential. According to Lucena (2005), it supplies approximately 80% of this coastal strip, including the capital, Natal.

The study area is located in the municipality of Nísia Floresta, in the southern coastal region of Rio Grande do Norte, along the left bank of the Boa Cica stream (Figure 1). This region, which already has a network of production and monitoring wells, is part of the Monsenhor Expedito Water Supply System, responsible for supplying approximately 300,000 inhabitants in the semi-arid region of the state (west of the study area). Initially, the well network was expected to provide a total discharge of approximately 900 m³/h, a figure that was not reached by the end of the project (with total available flow rates of 750 m³/h). This discrepancy is attributed to the local lithology, which is predominantly composed of fine and clayey sandstones (ALVES & LUCENA, 2021).

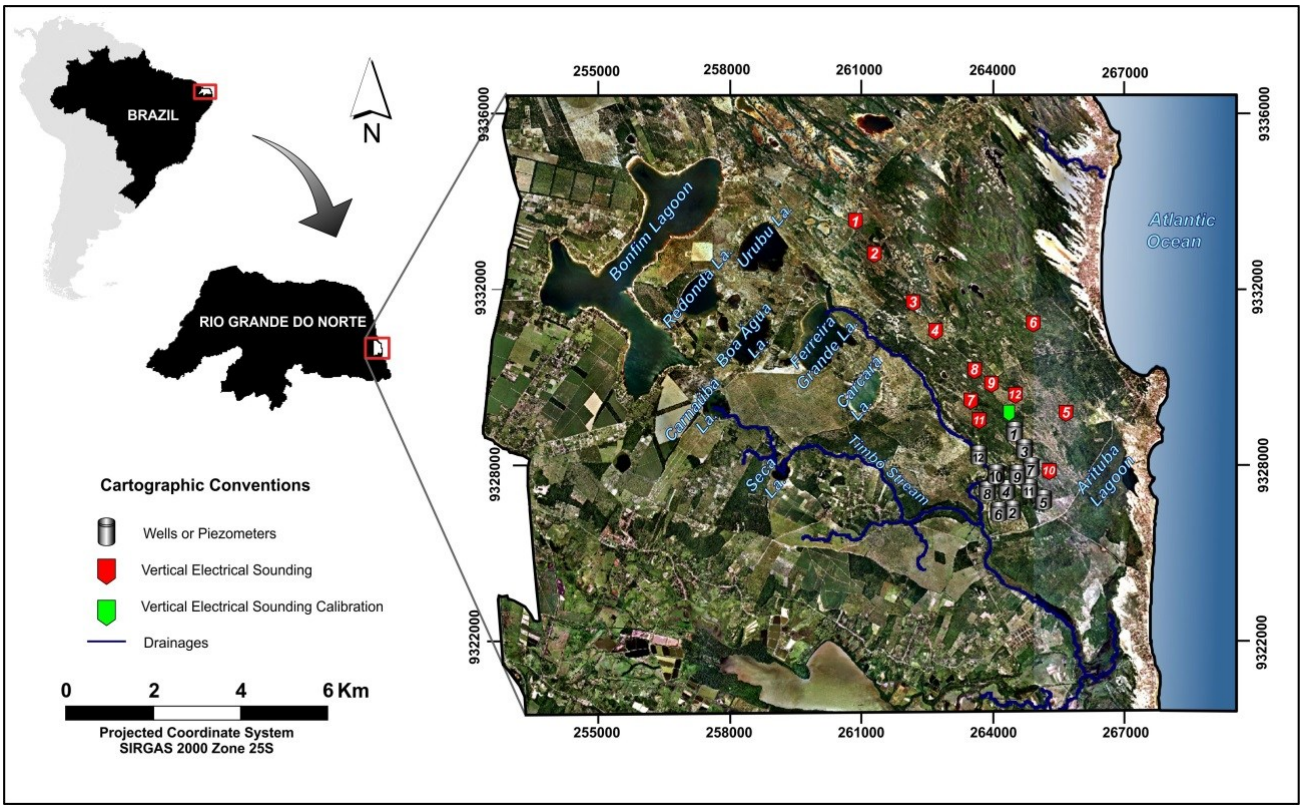

Figure 1 – Location of the study area, highlighting the lagoons that comprise the Bonfim Lacustrine System, as well as emphasizing the series of wells and VES on the left bank of the Boa Cica stream.
Source: Authors (2025).

Studies utilizing the Dar Zarrouk parameters (transverse electrical resistance and longitudinal conductance) highlight their applicability in different hydrogeological contexts. Patil et al. (2018) applied both parameters in the Chopda Taluka region (Maharashtra, India) and identified favorable zones for groundwater exploration. Souza et al. (2019) identified more promising hydrogeological subareas based on analyses of the transverse electrical resistance parameter. Silva and Lucena (2021) used transverse electrical resistance to estimate hydraulic transmissivity and, together with other geoelectrical data, evaluated the hydrogeological characteristics of an unconfined aquifer located in the eastern coastal region of Rio Grande do Norte. Additionally, these authors determined that the average resistivity of the saturated zone, rather than its average thickness, is the predominant factor in the composition of transverse electrical resistance in that specific area.

Ekanem (2022) investigated the hydrogeological behavior of an aquifer spanning five counties in Akwa Ibom State, southern Nigeria, applying correlation methods between electrical resistivity and hydraulic transmissivity to infer subareas with higher water productivity. Ikard et al. (2023) developed semi-empirical relationships between hydraulic transmissivity and average electrical resistivity to characterize the hydraulic properties of the Mississippi River Valley Alluvial Aquifer in the United States. Their study identified significant correlations between geoelectrical parameters, such as transverse electrical resistance, and transmissivity, highlighting promising regions for water exploration.

Given this context, the present research aims to develop an exploratory mapping of hydraulic transmissivity (T) within the hydrogeological framework of the Barreiras Aquifer. This will be achieved through data obtained from aquifer tests and calculations involving the geoelectrical parameter transverse electrical resistance (RT). Additionally, the study analyzes the predominant factor in the composition of RT—whether the average thickness or the average resistivity of the aquifer zone in the given context—to aid in identifying hydrogeologically promising areas.

2. Geological Context

The regional stratigraphy includes two lithostratigraphic sequences: one that does not outcrop, consisting of the Precambrian crystalline basement and Mesozoic sedimentary rocks, and another that outcrops, encompassing all Cenozoic-age sedimentation. The crystalline basement rocks, associated with the Caicó Complex, consist of gneisses, granites, migmatites, and granodiorites (LUCENA, 2005; SOUZA et al., 2019).

Unconformably overlying the crystalline basement are the Mesozoic sedimentary rocks, which, as reported, are divided into two units: a sandstone unit at the base and a carbonate unit with interbedded sandstones at the top. Both are associated with the Beberibe and Gramame-Maria Farinha Formations of the Pernambuco-Paraíba Coastal Basin (NOGUEIRA et al., 2006).

The outcropping sequence is characterized by sedimentary rocks of the Barreiras Formation and the Potengi Formation (Paleogene-Neogene), along with Quaternary sediments. These include the Barra de Tabatinga Unit, beachrocks, coastal deposits, fluvial deposits, multiple generations of dunes, mangrove and/or fluvial-lacustrine deposits, and sandy deposits (Figure 2) (ROSSETTI et al., 2013; LUCENA E SIMONATO, 2021).

The Barreiras Formation, which constitutes the first stratigraphic unit of the outcropping sequence and unconformably rests on the Mesozoic units of the region, presents a lithology that varies from base to top. It consists of medium to coarse sandstones, occasionally occurring in conglomeratic layers, together with sandy-clay or clayey-sandstone rocks. However, lateral facies variations occur in the sedimentary formation, both horizontally and vertically. The cliffs, which terminate abruptly along the coastline, are the most prominent outcrops of this formation (SOUZA et al., 2019; ALVES E LUCENA, 2021).

In this context, the basin is characterized by Neogene brittle deformation, represented by three main fault trends oriented at 040°-060° (NE-SW), 300°-320° (NW-SE), and 350°-010° (N-S), with the first two trends being predominant (BEZERRA et al., 2001; NOGUEIRA et al., 2006; SOUZA et al., 2019). A structural arrangement with dextral (NE-SW) and sinistral (NW-SE) movements were influenced by neotectonic stress fields (NUNES et al., 2020).

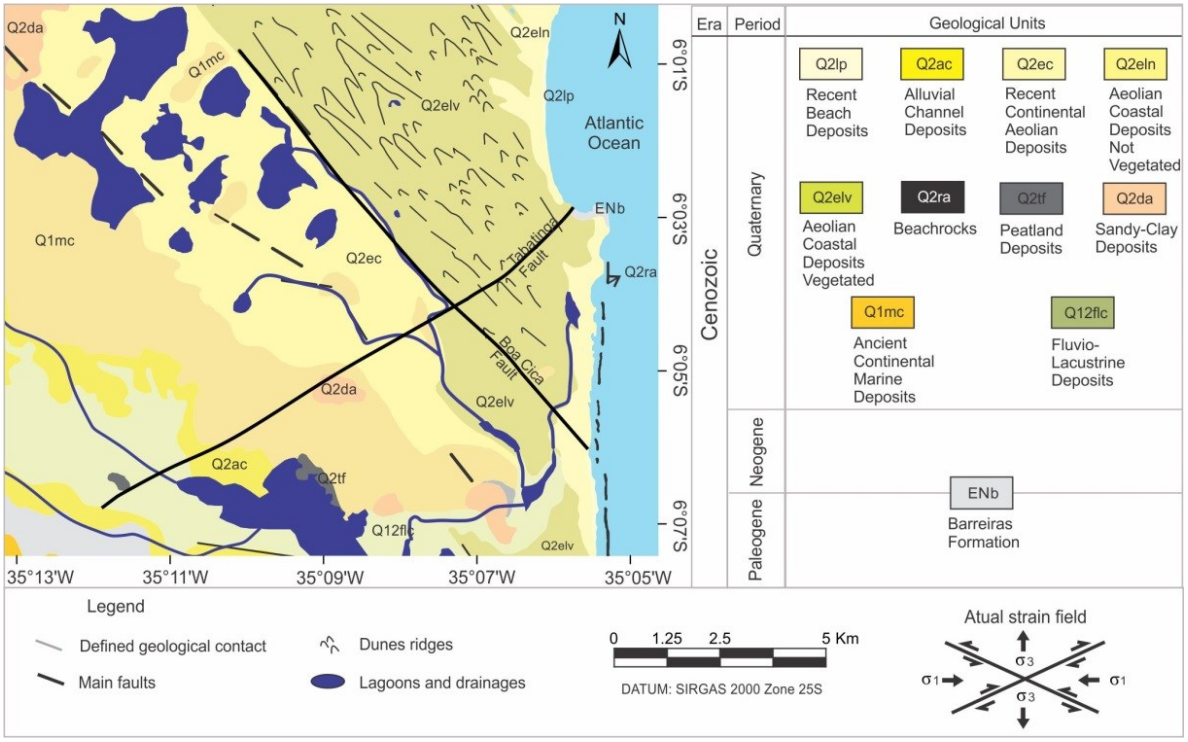

Figure 2 – Geological map of the region.
Source: Adapted from Alves and Lucena (2021).

These events and the reactivation of faulting led to the formation of structural blocks of the graben and horst types, associated with the uplift and subsidence of the hydrogeological basement (represented by the top of the Mesozoic carbonate sequence). This resulted in variations in the thicknesses of the overlying lithotypes. Such structural configuration influences the geometry of the Barreiras Aquifer and controls the region's drainage patterns (ALVES E LUCENA, 2021). Graben-type blocks can lead to greater saturated thicknesses and higher hydraulic transmissivities (SILVA E LUCENA, 2021).

Lucena and Queiroz (1996) reported a gravimetric anomaly of -4 mGal, described as the Papary Graben low, which influences the structural compartmentalization around the Boa Cica stream and the configuration of the Bonfim Lacustrine System, in addition to controlling the NE and NW lineaments. In the area, the main structural discontinuities are the Boa Cica Fault (NW-SE) and the Tabatinga Fault (NE-SW). The southwestern portion of the Papary Graben, located in Nísia Floresta, is delimited by the Boa Cica Fault, which is in contact with Quaternary covers and deposits of the Barreiras Formation (ALVES E LUCENA, 2021).

3. Hydrogeological Context

In the regional hydrogeological context, the eastern coast of Rio Grande do Norte is characterized by high rainfall, a flat to gently undulating relief, high infiltration rates, and water accumulation in rock formations. These factors result in significant groundwater resources, such as the Barreiras Aquifer, which supplies a substantial portion of the municipalities in this coastal strip (LUCENA, 2005).

The Barreiras Aquifer, named after the stratigraphic unit, consists of Cenozoic sedimentary rocks and exhibits a wide range of facies variations. At its base, medium to coarse sandstones predominate, with occasional conglomeratic layers. At the top, sandy-clay or clayey-sandstone rocks are present. Although generally classified as an unconfined aquifer, localized semi-confinements can occur due to the presence of clayey or silty layers (SOUZA et al., 2019; NUNES et al., 2020).

Quaternary sediments, mainly of eolian origin, overlie the Barreiras Aquifer and function as rainfall transmitters, allowing infiltration and recharge of the aquifer (ALVES E LUCENA, 2021). The role of dunes in this process creates a

unique hydraulic system, sometimes referred to as the Dunas-Barreiras Aquifer System (MELO et al., 1994). Beneath the sedimentary rocks of the Barreiras Formation, forming the aquifer's base, there are Mesozoic calciferous sandstones to argillites, which act as an aquitard due to their hydrodynamic properties (SILVA et al., 2014).

The Barreiras Aquifer exhibits local hydraulic transmissivities (T) in the range of 10^{-4} to 10^{-2} m²/s and hydraulic conductivities (K) around 10^{-4} m/s, values obtained from aquifer tests (ALVES E LUCENA, 2021). The observed discharges in the studied well field reach individual flow rates of up to 100 m³/s.

Effective porosities have been estimated at around 10% (ALVES et al., 2016). However, through thin-section analysis, Silva et al. (2014) determined effective porosities of 7.6%. Lucena et al. (2016) found effective porosities above 11% in similar sandstones in nearby regions, despite their Mesozoic age. This assessment was conducted through computational analysis of images obtained from thin sections.

4. Methodology

Among the various geophysical methods used in groundwater investigations, geoelectrical methods are widely applied, particularly the electrical resistivity method, which provides significant reach both vertically and horizontally (ORELLANA, 1972; BRAGA, 2016).

This study was based on data from electrical resistivity surveys, employing the vertical electrical sounding (VES) technique with a Schlumberger electrode array (ORELLANA, 1972). The geoelectrical data acquisition consists of a four-electrode configuration (AMNB), where electrodes A and B are responsible for injecting electrical current (I) into the ground, generating an electric field that flows through the subsurface in the form of equipotential lines. Two potential electrodes, designated M and N, measure the potential difference (ΔV) created by the electric flow (ORELLANA, 1972; BRAGA, 2016).

Thus, the electrical resistivity (ρ) can be calculated using the arrangement of these four electrodes, known as the geometric coefficient K, through equation 1.

$$\rho = K \frac{\Delta V}{I} \tag{1}$$

The development of the Vertical Electrical Sounding (VES) technique involves the symmetrical displacement of the current electrodes (A and B) in opposite directions relative to a fixed central point, located between the potential electrodes (M and N). This arrangement allows for analysis at different depths (ORELLANA, 1972; KOEFOED, 1979).

The field data were reinterpreted using the IPI2Win geoelectric inversion software, version 2.1, developed by Geoscan-LTDA (BOBACHEV et al., 2000).

A geoelectric calibration survey was conducted to provide lithological and hydrogeological information in areas with unknown well profiles and to assist in quantitatively interpreting geoelectric soundings. This calibration involves surveys adjacent to wells with known hydrostratigraphic profiles, correlating lithological descriptions and layer thicknesses with the obtained geoelectric data. Based on the inverse model and the adjustment between the modeled curve and field data, the layer thickness values are established, and the resistivity values are obtained. These results are then associated with other VES data to more accurately interpret the geoelectric layers (BRAGA, 2016; SOUZA et al., 2019).

Assuming a geoelectric section with a thickness E_i and resistivity ρ_i, as illustrated in the hypothetical geoelectric prism in Figure 3, the electrical current introduced into the bedrock will flow along two preferential paths: one perpendicular and the other parallel to the stratification. However, given the objectives of this study, only the perpendicular flow to stratification will be considered. In this case, the various layers act as conductors in series, leading to the summation of their respective resistances (ORELLANA, 1972; BRAGA, 2016; SILVA & LUCENA, 2021).

Thus, considering L as the length and S as the cross-sectional area, the expression for the electrical resistance of a given layer ii is given by Equation 2.

$$R_i = \rho_i \frac{L}{S} = \rho_i \frac{E_i}{1x1} = \rho_i E_i \tag{2}$$

This product is called unit transverse resistance (RT), with its unit of measurement given in Ohm·m², while electrical resistivity is given in Ohm·m, and the thickness of the saturated layer in meters.

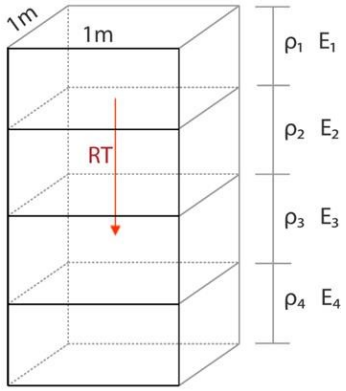

Figure 3 – Prism indicating the flow of electric current in the bedrock.
Source: Adapted from Silva and Lucena (2021).

In this context, the average thickness, average resistivity, and transverse electrical resistance of the saturated zone were calculated for each VES. The average thickness was determined by summing the layers that make up the saturated zone, as shown in Equation 3.

$$E_S = \sum E_i \tag{3}$$

The average resistivity of the saturated zone, in turn, was determined using the weighted average of the mean resistivities, with the average thickness of the saturated zone as the weighting factor.

$$\rho_m = \frac{RT}{E} \tag{4}$$

The calculation of transverse electrical resistance was performed individually for each geoelectric layer, and then the sum of these layers was taken to cover the entire saturated zone, as indicated by Equation 5 (BRAGA, 2016; SILVA & LUCENA, 2021).

$$\mathrm{RT} = \sum \rho_i E_i \tag{5}$$

Hydraulic transmissivity (T) represents the amount of water that can be transmitted horizontally through the entire thickness of the aquifer. Equation 6 algebraically characterizes the concept of this parameter (FEITOSA et al., 2008).

$$\mathrm{T} = \mathrm{K.E} \tag{6}$$

Where hydraulic transmissivity (T) is represented in m²/s, and the parameters K and E denote hydraulic conductivity and saturated thickness, given in m/s and m, respectively.

Hydraulic conductivity indicates the ability of the rock material to allow water flow through it. The higher the hydraulic conductivity, the more easily water can move within the substrate. In this context, the parameters of electrical resistivity and hydraulic conductivity are intrinsically correlated in a direct relationship. For example, saturated sandstones exhibit higher resistivities and hydraulic conductivities compared to siltstones. Therefore, due to the direct relationship between these parameters, transverse electrical resistance and hydraulic transmissivity (Equations 5 and 6) are also proportional, considering the same saturated thickness in both equations (SILVA & LUCENA, 2021; IKARD et al., 2023).

The data related to aquifer tests were retrieved from SEMARH (2012) and referred to pumping tests conducted on the twelve production wells of the local water supply system, using four to six observation wells in each procedure. The pumping tests involved fixed flow rates ranging from 39.79 to 60.01 m³/h, lasting 48 hours, plus 6 hours of recovery of dynamic levels. The results were interpreted using the De Glee method, considering a steady-state flow regime (FEITOSA et al., 2008).

The transmissivity value obtained at well PZ3-PS01, the same used for geoelectric calibration, was 1.58×10^{-3} m²/s. Using this value along with the transverse electrical resistance obtained from the calibration VES (VEScal-13), it was possible to estimate hydraulic transmissivities for the remaining 12 VES locations. Combined with the data acquired from the wells, this allowed for the development of a preliminary exploratory hydraulic transmissivity map.

Additionally, an analysis was conducted to determine which of the parameters involved in transverse electrical resistance is dominant, using the least squares method. This method establishes a linear correlation between two variables, plotted along the X and Y axes, through a simple linear regression. The process generates a correlation factor (R^2) in its trend lines, based on the equation of a straight line (Equation 7), where values closer to 1 indicate stronger correlations (SILVA & LUCENA, 2021).

$$Y = aX + b \tag{7}$$

Where X represents the independent variable, indicated by either the average electrical resistivity or average thickness, both parameters of the saturated zone, while Y represents the transverse electrical resistance, denoting the dependent variable.

To display the parameters of transverse electrical resistance and hydraulic transmissivity, the cartographic representations were generated using geostatistical methods and interpolation and gridding techniques (kriging), within a GIS environment using the ArcGIS software (CHISTAKOS, 2000; SOUZA et al., 2019).

5. Results and discussions

The geoelectric calibration was performed approximately at the center of the Boa Cica catchment area and adjacent to well PZ3-PS1 (Figure 4A). This geoelectric survey (SEVCal-13) revealed resistivity intervals ranging from 320 to 930 Ohm.m, along with a 17-meter thickness (confirmed by measuring the water level at the mentioned catchment) for the unsaturated zone, indicating the presence of surface moisture. Three geoelectric layers were identified in the saturated zone, with resistivities of 360, 40, and 200 Ohm.m and thicknesses of 9, 5, and 57 meters, respectively, from top to base (Figure 5).

Resistivity values around 360 Ohm.m are associated with sandy-clayey rocks (relatively higher hydraulic conductivity), with a gradual increase in sand content proportional to the increase in resistivity. Meanwhile, values equal to or lower than 200 Ohm.m are linked to more clayey rocks (lower hydraulic conductivity), including more characteristic argillites (40 Ohm.m). The base of the geoelectric model shows a resistivity of 1900 Ohm.m, revealing a strong influence of purer carbonate rocks from the Mesozoic hydrogeological basement of the Barreiras Aquifer, in contrast to calcareous sandstones and argillites at the base of the hydrostratigraphic profile (whose thickness is not significant in the inverse SEV model).

It is worth noting that a better physical-mathematical curve fit was sacrificed in favor of better incorporating local hydrogeological constraints. Table 1 presents the field data related to the geoelectric calibration survey conducted adjacent to PZ3-PS1 in the CAERN catchment area in Boa Cica. Figure 4B displays the graph of the aquifer test carried out at the mentioned well, in which a hydraulic transmissivity value of 1.58×10^{-3} m²/s was obtained using the De Glee method.

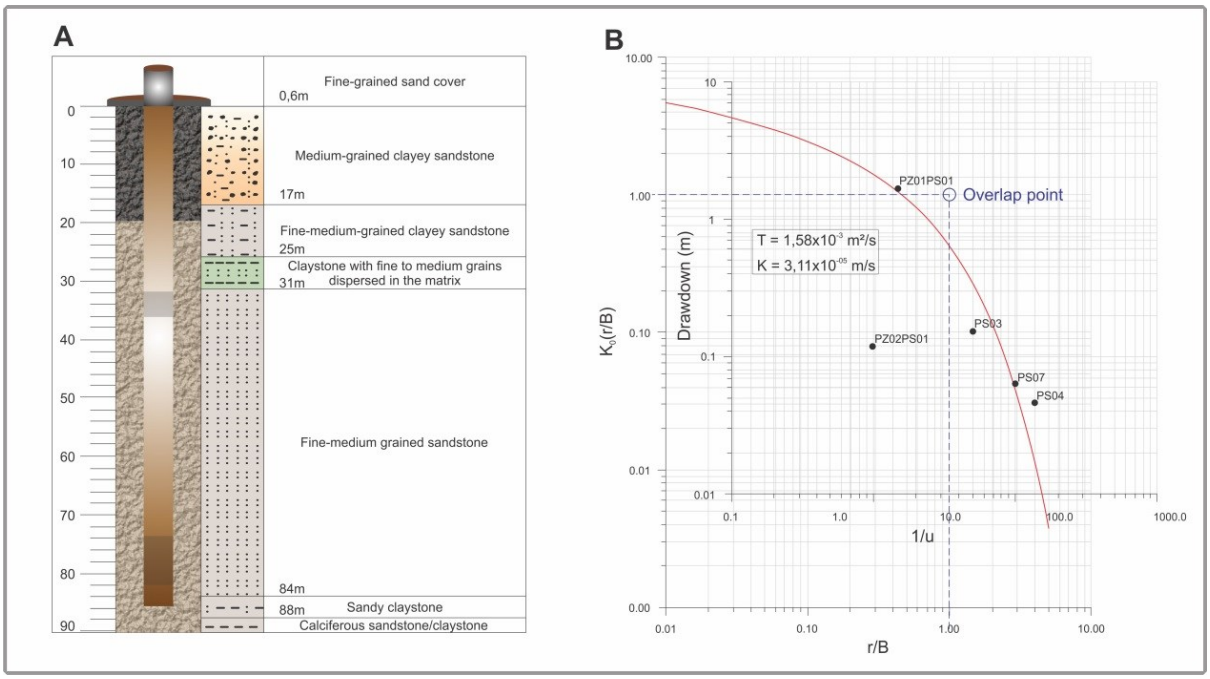

Figure 4 – Simplified lithological-construction profile of well PZ3-P01 (A); graph of the aquifer test conducted at the mentioned well using the De Glee method (B).
Source: Authors (2025).

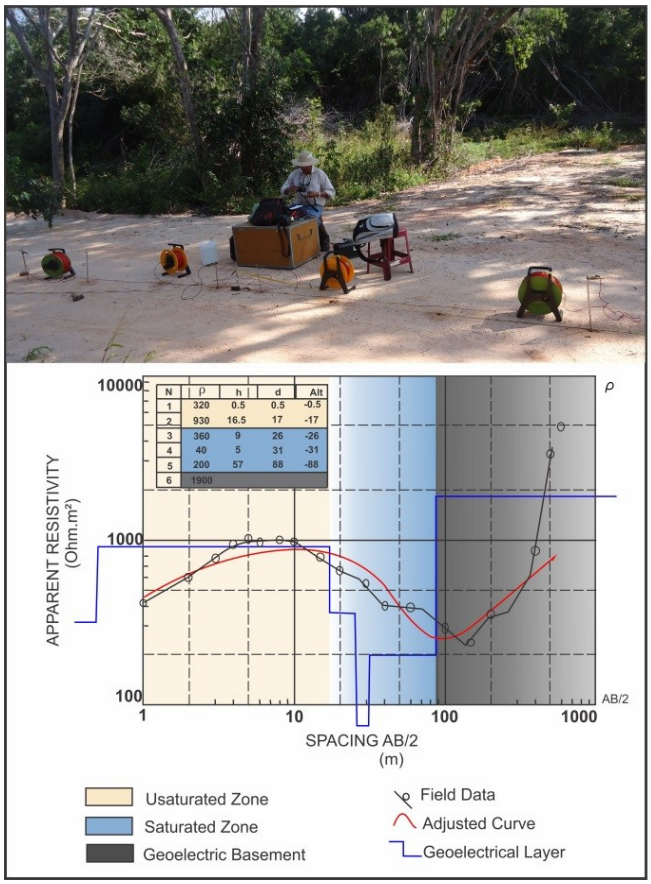

Figure 5 – Calibration electrical sounding (SEVcal-13), showing the fit of the modeled curve (in red) to the field data (in black).
Source: Authors (2025).

Figures 6A and 6B present two other SEVs performed (see Figure 1), emphasizing the procedure for adjusting the field curves to the modeled ones, as well as the interpreted geoelectric models.

Table 1 – Vertical electrical soundings conducted in the area of the left bank of the Boa Cica stream, with the respective saturated and unsaturated thicknesses, in addition to the average resistivity and transverse electrical resistance derived from the interpreted geoelectric models.

VES's	Coordinates		Elevation (m)	Unsaturated Thickness (m)	Saturated Thickness (m)	Transv. Elec. Resistance (Ohm.m²)
	UTM X	UTM Y				
VES 1	260850	9333570	40.97	3.5	54.0	16864
VES 2	261277	9332831	44.70	1.3	62.5	24500
VES 3	262169	9331704	41.12	20.0	65.2	22168
VES 4	262670	9331074	42.19	4.5	72.0	58680
VES 5	265664	9329193	25.93	12.0	80.0	18800
VES 6	264920	9331242	37.89	3.7	65.0	7220
VES 7	263687	9329015	38.22	8.8	71.8	45593
VES 8	263575	9330192	32.39	4.5	59.5	23734
VES 9	263940	9329868	35.77	3.6	47.0	28859

VES 10	265120	9327858	22.46	7.0	50.3	24903
VES 11	263499	9329502	33.22	8.7	60.7	35509
VES 12	264496	9329556	37.38	9.0	65.6	40219
VESCal 13	264439	9329096	37.43	17.3	70.6	14840

Source: Authors (2025).

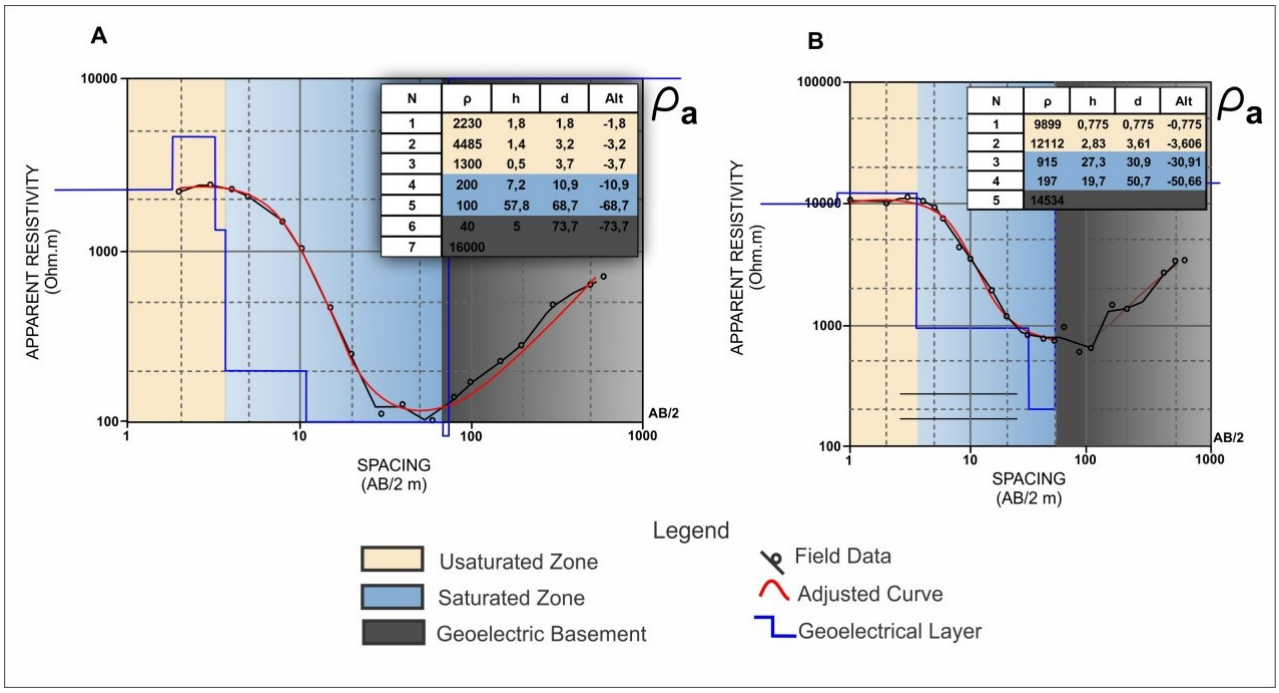

Figure 6 – SEVs 6 and 9 (A and B, respectively), emphasizing the fit of the apparent resistivity curves, as well as the respective geoelectric models.
Source: Authors (2025).

Based on the calculated values of average thickness, average resistivity, and transverse electrical resistance across the entire saturated zone, the spatial distribution of these results was analyzed. Figure 7 presents the transverse electrical resistance (RT) map obtained through interpolation and gridding, as reported.

In general, the transverse electrical resistance (RT) values ranged from 7,220 Ohm.m² to 56,680 Ohm.m², with a median of 24,500 Ohm.m². The average resistivity of the saturated zone (ρ_m) ranged from 111 Ohm.m to 815 Ohm.m, with a median of 399 Ohm.m. The saturated thickness, however, varied between 47 m and 80 m, with a median of 65 m.

The correlation and analysis of the predominant factor between thickness and average resistivity—both from the saturated zone, which together compose the transverse electrical resistance—revealed linear regression (R^2) values of 0.03 and 0.89 for thickness and average resistivity, respectively. The graph included in Figure 7 illustrates the process performed, highlighting the relationship between the average resistivity of the saturated zone and Transverse Electrical Resistance (RT).

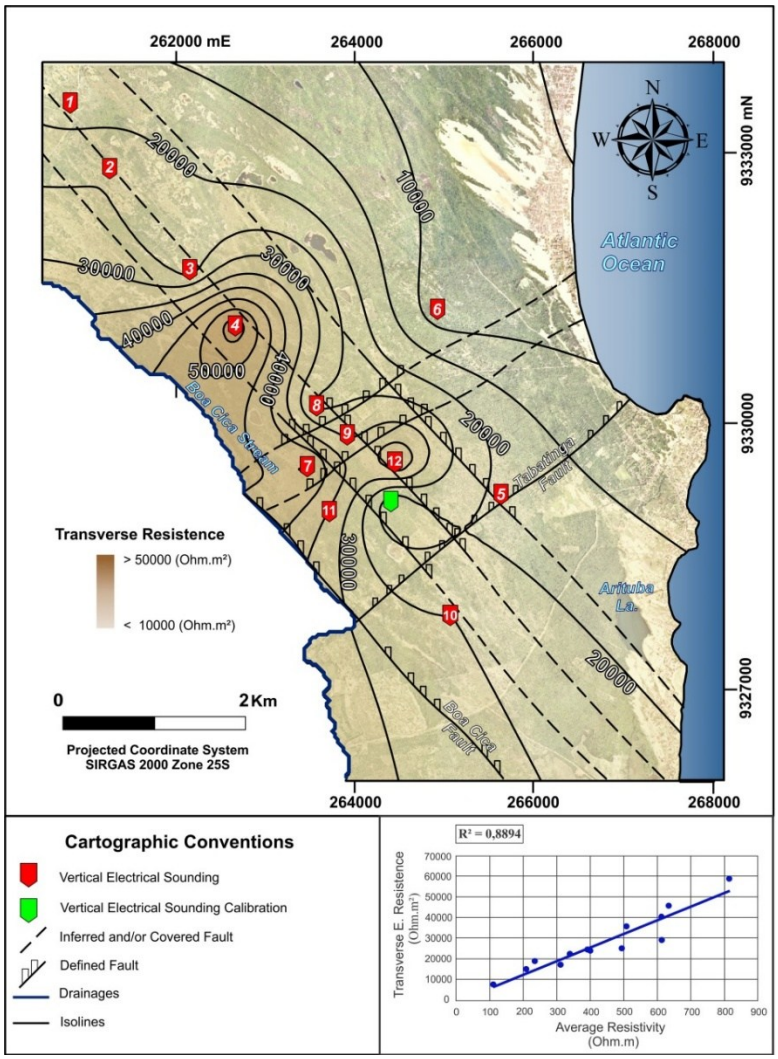

Figure 7 – Transverse electrical resistance map and the RT vs. average resistivity graph of the saturated zone.
Source: Authors (2025).

Analyzing the transverse electrical resistance mapping of the saturated zone (Figure 7), it is observed that the highest values occur in the southern and western portions, around SEVs 4, 7, 9, 11, and 12, with values reaching up to 58,680 Ohm.m². Therefore, these subareas are identified as the most promising in terms of hydrogeological potential.

The results obtained between RT and the average resistivity of the saturated zone show similarities, as the highest values of these parameters were also recorded in the southern and western portions of the area. This similarity is further confirmed in the dependency analysis, where the correlation factor (R^2) between these parameters is significantly higher compared to the correlation between average thickness and RT. Thus, it is indicated that the average electrical resistivity of the saturated zone is the predominant factor in the RT calculation, allowing the inference that the most promising hydrogeological potential areas are associated with higher average resistivity values of the saturated zone.

In this context, it is noteworthy that, although the Barreiras Aquifer presents structural compartmentalization at a regional scale (SOUZA et al., 2019; NUNES et al., 2020; ALVES & LUCENA, 2021), in the current study area, the lithological composition with finer granulometry, associated with lower resistivity values, plays a predominant role in local hydraulic transmissivities and, consequently, in transverse electrical resistances.

Table 2 presents the results of hydraulic transmissivity (T) estimates, obtained through the direct relationship between RT and T and from aquifer tests. Analyzing the distribution of interpolated results, it is noted that the regions

with the highest hydraulic transmissivity values are located in the southern and western portions (Figure 8). These results align with those obtained in the transverse electrical resistance calculations, showing their highest values in the same respective areas. The transmissivity values (T) ranged from 0.76×10^{-3} m²/s to 9.96×10^{-3} m²/s, with a median of 2.58×10^{-3} m²/s.

Table 2 – Summary of hydraulic transmissivity values obtained by SEMARH (2012) for the twelve (12) original production wells (PS) of the Boa Cica area, in addition to those estimated for the surroundings of VES 1 to 12 and the calibration VES 13 (VEScal).

Well/VES	Coordinates		T (m²/s) x 10^{-3}
	UTM X	UTM Y	
PS 01	264.452	9.328.912	1.58
PS 02	264.398	9.327.116	3.26
PS 03	264.696	9.328.472	1.56
PS 04	264.249	9.327.545	3.70
PS 05	265.152	9.327.243	3.68
PS 06	264.172	9.327.125	2.33
PS 07	264.875	9.328.005	1.74
PS 08	263.863	9.327.543	9.96
PS 09	264.611	9.327.747	2.41
PS 10	264.077	9.327.845	3.25
PS 11	264.775	9.327.554	2.58
PS 12	263.720	9.328.250	2.45
VES 1	260.850	9.333.570	1.79
VES 2	261.277	9.332.831	2.61
VES 3	262.169	9.331.704	2.36
VES 4	262.670	9.331.074	6.25
VES 5	265.664	9.329.193	2.01
VES 6	264.920	9.331.242	0.76
VES 7	263.499	9.329.502	4.85
VES 8	263.575	9.330.192	2.53
VES 9	263.940	9.329.868	3.07
VES 10	265.113	9.327.858	2.65
VES 11	263.687	9.329.015	3.78
VES 12	264.496	9.329.556	4.28
VEScal	264.439	9.329.096	1.58

Source: Authors (2025).

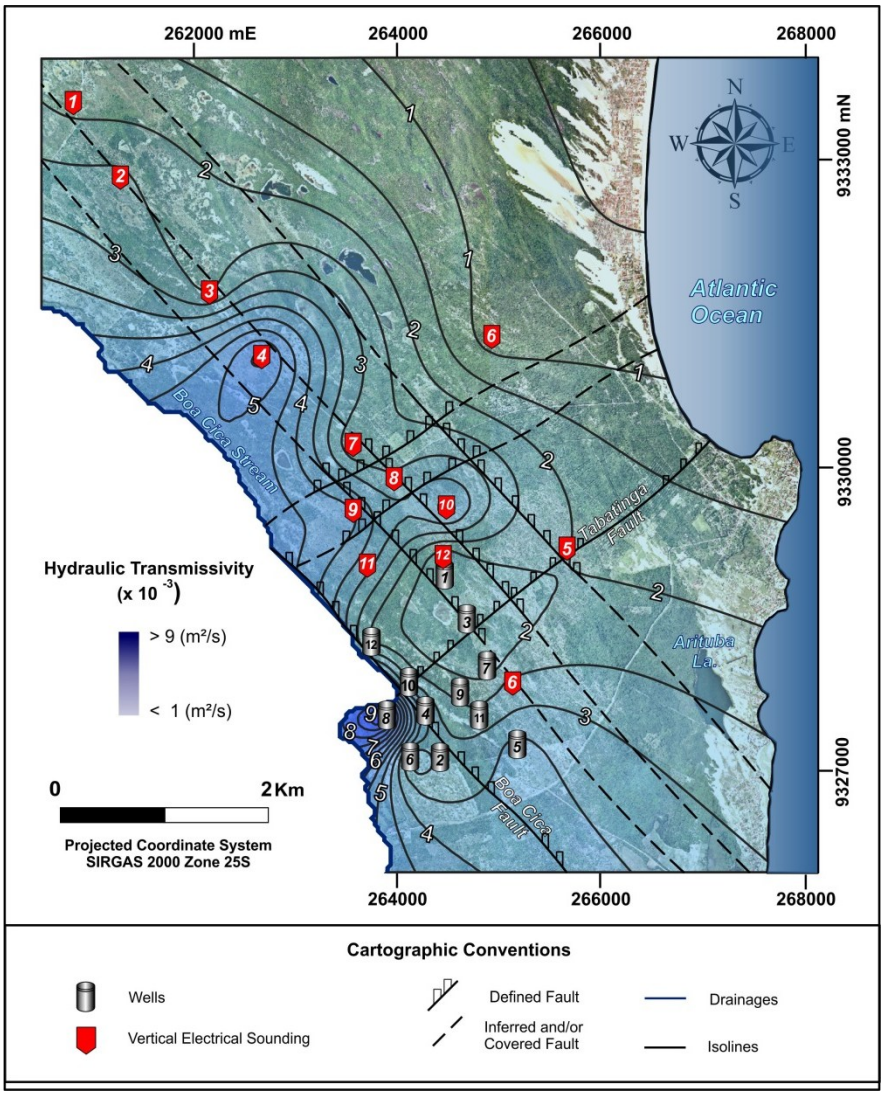

Figure 8 – Hydraulic transmissivity estimates using combined transverse electrical resistance and well data.
Source: Authors (2025).

The joint analysis of the maps in Figures 7 and 8 (transverse electrical resistance and hydraulic transmissivity, respectively) highlights their convergence, supported by prior geoelectric calibration, particularly between "RT" and "T". This direct correlation between these parameters is crucial when estimating hydraulic transmissivity in areas with limited well data available.

However, the hierarchical analysis between resistivity and average thickness requires more extensive studies on the Barreiras Aquifer, given the divergent results in different occurrence areas. In certain contexts, average resistivity may have a greater influence than the average saturated thickness, especially in clean sandstone formations with higher hydraulic conductivity. On the other hand, relatively greater saturated thicknesses may indicate low hydrogeological potential due to the presence of clay-rich sequences.

Therefore, a detailed spatial analysis of the distribution of transverse electrical resistance values, as well as the parameters that compose it, should be considered in advance for each hydrogeological context. This approach helps to identify areas with higher potential for groundwater exploration.

6. Conclusions

Alternative hydrogeophysical approaches are essential for filling knowledge gaps in regions with few or no well data. The application of the geoelectric method, particularly in calculations involving transverse electrical resistance (RT) through calibrated inverse interpretative models, allows for the evaluation of promising zones for future water extraction, especially in the context of shallow aquifers. Therefore, this methodology was employed to optimize the identification of favorable areas for groundwater exploitation in the region along the left bank of the Boa Cica stream, located in the municipality of Nísia Floresta-RN State, Brazil.

The success of using the RT parameter stems not only from its non-invasive data acquisition but also from its direct relation to two key parameters of the saturated zone: thickness and average resistivity. The latter is directly linked to hydraulic conductivity, which is a fundamental component of hydraulic transmissivity (T). Due to this proportionality, clean sandstone formations exhibit higher electrical resistivity and hydraulic conductivity, whereas rock formations with high clay content tend to show lower values.

The T estimates, obtained both from aquifer tests and through RT-based calculations, calibrated using prior geoelectric surveys, identified the southern and western portions of the study area as the high-exploration potential zones, with values reaching up to 9.96×10^{-3} m²/s. The RT results corroborate this direct relationship, as the highest RT values were also observed in these subareas, reaching 58,680 Ωm², confirming them as the most promising zones in terms of hydrogeological potential.

These findings highlight the effectiveness of the adopted methodology in estimating T values derived from RT, leading to the preliminary development of an exploratory hydraulic transmissivity map. This approach provides critical support for regions with limited or no well data, particularly for guiding public management strategies aimed at sustainable groundwater resource management and exploration.

The linear regressions generated to assess the degree of influence between thickness and average resistivity of the saturated zone, which together constitute the RT parameter in the context of the Barreiras Aquifer for the study area, revealed a correlation factor of $R^2 = 0.89$ for average resistivity, which is significantly higher than that of average thickness. This result demonstrates that average resistivity of the saturated zone predominantly controls the RT calculation, as evidenced by the similarity between the interpolated results for both parameters.

However, this result should not be considered absolute for the entire aquifer, as a previous study within the same hydrogeological context found that average saturated thickness exerted a greater influence than average resistivity.

Given these findings, it is recommended to expand these analyses to other regions where the Barreiras Aquifer occurs. The goal is to obtain a broader trend regarding the predominance of either thickness or average resistivity in aquifer characterization. Since resistivity is directly linked to hydraulic conductivity, its role in transverse electrical resistance (RT) calculations is crucial for identifying hydrogeologically promising subareas.

Acknowledgments

"This study was carried out with the support of the Coordination for the Improvement of Higher Education Personnel (CAPES) – Brazil, under Funding Code 001." The authors thank the Water and Sewage Company of Rio Grande do Norte (CAERN) for sharing well data.

References

ALVES, R. S., MELO, J. G., SILVA, C. T. X. L., OLIVEIRA, C. C. C. *Recursos Hídricos Subterrâneos da Região de Parnamirim, RN: uso das águas e potencialidades*. Revista Águas Subterrâneas, v. 30, p. 37-52, 2016. https://doi.org/10.14295/ras.v30i1.28486.

ALVES, R. S., LUCENA, L. R. F. *Uso de dados hidrogeofísicos e modelos numéricos como alternativa na otimização de locação de poços em um aquífero não confinado.* Revista Águas Subterrâneas, v. 35, n. 1, p. 51-64, 2021. http:/dx.doi.org/10.14295/ras.v35i1.29987.

BEZERRA, F. H. R., AMARO, V.E., VITA-FINZI, C., SAADI, A. *Pliocene-quaternary fault control of sedimentation and coastal plain morphology in NE Brazil.* Journal of South American Earth Sciences. 14:61-75, 2001. doi 10.1016/S0895-9811(01)00009-8.

BOBACHEV, A. A., MODIN, I. N., SHEVNIN, V. A. IPI2Win v. 2.1, IPI_RES2, IPI_RES3, *User's Guide*. Geoscan-M Ltd, 2000.

BRAGA, A.C.O. *Geofísica aplicada: métodos geoelétricos em hidrogeologia*. Oficina de textos. 157 p, 2016.

CHRISTAKOS, G. *Modern Spatiotemporal Geostatics*. New York: Oxford Univ. Press, 312 p, 2000.

EKANEM, A. M. *Georesistivity modelling and mapping of aquifer geometry and hydraulic characteristics in a sedimentary environment*. Water Conservation Science and Engineering, v. 7, n. 4, p. 585-598, 2022. https://doi.org/10.1007/s41101-022-00166-9.

FEITOSA, F. A. C., MANOEL FILHO, J., FEITOSA, E. C., DEMETRIO, J. G. A. *Hidrogeologia - conceitos e aplicações*. 3a ed. rev. CPRM: LABHID, Rio de Janeiro, 2008.

IKARD, S. J., MINSLEY, B. J., RIGBY, J. R., KRESS, W. H. *A model of transmissivity and hydraulic conductivity from electrical resistivity distribution derived from airborne electromagnetic surveys of the Mississippi River Valley Alluvial Aquifer, Midwest USA.* Hydrogeology Journal, v. 31, n. 2, p. 313-334, 2023. https://doi.org/10.1007/s10040-022-02590-6.

KOEFOED, O. *Geosouding Principles, 1: Resistivity Souding Measurements*. ElVESier Scientific Publishing Company, Amsterdam, Oxford, New York, 1979.

LUCENA, L. R. F., QUEIROZ, M. A. *Considerações sobre as influências de uma tectônica cenozóica na pesquisa e prospecção de recursos hídricos - o exemplo do litoral sul de Natal-RN, Brasil.* Revista Águas Subterrâneas, São Paulo, v. 1, n. 15, p. 81-88, 1996. https://doi.org/10.14295/ras.v15i1.28579.

LUCENA, L. R. F. *Implicação da compartimentação estrutural no Aquífero Barreiras na área da bacia do Rio Pirangi – RN.* Tese (Doutorado) – Universidade Federal do Paraná, Programa de Pós-Graduação em Geologia, Curitiba-PR, 2005.

LUCENA, L. R. F., DA SILVA, L. R. D., VIEIRA, M. M., CARVALHO, B. M., XAVIER JÚNIOR, M. M. *Estimating hydraulic parameters of Açu-Brazil aquifer using the computer analysis of micrographs.* Journal of Hydrology, v. 535, p. 61-70, 2016. https://doi.org/10.1016/j.jhydrol.2016.01.025.

LUCENA, L. R. F., SIMONATO, M. D. *Considerações Sobre a Conexão Hidráulica de um Aquífero Não Confinado em Zonas de Falhas a Partir de Dados Isotópicos, NE/Brasil.* Geo-Ambiente Online, Revista Eletrônica do Curso de Geografia Graduação e Pós-graduação, n. 40, maio-agosto, 2021.

MELO, J. G., REBOUÇAS, A. C., QUEIROZ, M. A. *Análise dos componentes hidrogeológicos da área de Natal – RN.* In: CONGRESSO BRASILEIRO DE ÁGUAS SUBTERRÂNEAS, VIII. Anais. Recife, Associação Brasileira de Águas Subterrâneas. 471-480, 1994.

NOGUEIRA, F. C. C., BEZERRA, F. H. R., CASTRO, D. L. *Deformação Rúptil em Depósitos da Formação Barreiras na Porção Leste da Bacia Potiguar.* Geologia USP-Série Cientifica. v.6, n. 2, p. 51-59, 2006. doi 10.5327/S1519-874X2006000300007.

NUNES, L. M. G., LUCENA, L. R. F., SILVA, C. C. N. *Reserve evaluation of a faultconditioned aquifer: the Barreiras Aquifer in the coastal region of NE Brazil.* Brazilian Journal of Geology, v. 50, n. 1, p. e20180127, 2020. https://doi.org/10.1590/2317-04889202020180127.

ORELLANA, E. *Prospecion geoeletrica en corriente continua*. Ed. Paraninfo, Madrid. 523 p., 1972.

PATIL, S. N., KACHATE, N. R., INGLE, S. T. *Estimation of Dar-Zarrouk Parameters for Groundwater Exploration in Parts of Chopda Taluka, Jalgaon district, Maharashtra (India).* J. Ind. Geophys. Union, v. 22, n. 4, p. 425-435, 2018.

ROSSETTI, D. F., BEZERRA, F. H. R., DOMINGUEZ, J. M. L. *Late Oligocene – Miocene transgressions along the equatorial and eastern margins of Brazil.* Earth-Science Reviews, v. 123, p. 87–112, 2013. https://doi.org/10.1016/j.earscirev.2013.04.005.

SEMARH. *Estudo Hidrodinâmico com Modelagem Numérica para Definição das Condições de Explotação - Projeto Executivo das Subadutoras para Suprimento do Reservatório de Reunião dos Poços da Área Boa Cica para Reforço do Suprimento da Adutora Monsenhor Expedito.* Secretaria de Estado do Meio Ambiente e dos Recursos Hídricos, TECHNE-Engenheiros Consultores. SEMARH, Natal. 147 p., 2012.

SILVA, L. R. D., LUCENA, L. R. F., VIEIRA, M. M., NASCIMENTO, A. F. *Estimativa de parâmetros hidráulicos do Aquífero Barreiras-RN a partir de análise computacional de 51 imagens de lâminas delgadas*. Águas Subterrâneas, v. 28, n. 2, p. 14-27, 2014. https://doi.org/10.14295/ras.v28i2.27873.

SILVA, J. V., LUCENA, L. R. F. *Estimativas de potencialidades hidrogeológicas em um aquífero não confinado a partir do parâmetro resistência elétrica transversal.* Águas Subterrâneas, v. 35, n. 3, e-30092, 2021. http:/doi.org/10.14295/ras.v35i3.30092.

SOUZA, I. V. F., LUCENA, L.R.F., BEZERRA, F. H. R., FILHO, J. B. D. *Use of hidrogeophysical data to determine the role of faults in the geometry of the Barreiras Aquifer, Brazil. Brazilian* Journal of Geology, v. 49, n. 2, p. e20170141, 2019. http://doi.org/10.1690/2317-4889201920170141.